Available online at www.sciencedirect.com

ScienceDirect

Physics Letters B 650 (2007) 331–336

PHYSICS LETTERS B

www.elsevier.com/locate/physletb

Wobbling excitations at high spins in $A \sim 160$

J. Kvasil [a], R.G. Nazmitdinov [b,c,*]

[a] *Institute of Particle and Nuclear Physics, Charles University, V. Holešovičkách 2, CZ-18000 Praha 8, Czech Republic*
[b] *Departament de Física, Universitat de les Illes Balears, E-07122 Palma de Mallorca, Spain*
[c] *Bogoliubov Laboratory of Theoretical Physics, Joint Institute for Nuclear Research, 141980 Dubna, Russia*

Received 11 March 2007; received in revised form 8 May 2007; accepted 18 May 2007

Available online 24 May 2007

Editor: W. Haxton

Abstract

We found that in ^{156}Dy and ^{162}Yb the lowest odd spin gamma-vibrational states transform to the wobbling excitations after the backbending, associated with the transition from axially-symmetric to nonaxial shapes. The analysis of quadrupole electric transitions determines uniquely the sign of the γ-deformation in both nuclei after the transition point.

PACS: 21.10.Re; 21.60.Jz; 27.70.+q

Thanks to novel experimental detectors, a new frontier of discrete-line γ-spectroscopy at very high spins has been opened in the rare-earth nuclei (see, for example, [1]). These nuclei can accommodate the highest values of the angular momentum, providing one with various nuclear structure phenomena. The quest for manifestations of nonaxial deformation is one of the driving forces in high spin physics in past few years [2]. The identification of wobbling excitations is recognized nowadays as a convincing proof of the nonaxiality. Wobbling excitations were suggested first by Bohr and Mottelson for rotating even–even nuclei [3] and studied soon within simplified microscopic models [4] (see also Ref. [5] and references therein). According to the microscopic approach [6,7], the wobbling excitations are vibrational states of the negative signature built on the positive signature yrast (vacuum) state. Their characteristic feature is collective E2-transitions with $\Delta I = \pm 1\hbar$ between these and yrast states. First experimental evidence of such states in odd Lu nuclei was reported only recently [8].

The first analysis of the properties of the second triaxial superdeformed band in ^{163}Lu was based upon phenomenological particle-rotor calculations [9]. The absolute values of the irrotational moments of inertia were fitted and so-called "γ-reversed" dependence of these moments was introduced in order to obtain a reasonable agreement with the experimental data. It was shown in Ref. [10] that the microscopic approach [7] may gain a better insight into the observed phenomena. In the analysis of [10], however, the constant mean-field deformation parameters are used, which is not always justified. Moreover, the authors admitted that the kinematic moment of inertia $\Im_x$ was not described properly due to the strong velocity dependence of the Nilsson potential (see discussion in Ref. [10]). We recall that wobbling excitations depend on all three moments of inertia that characterize the nonaxial shape. Therefore, a self-consistent description of moments of inertia is a prerequisite of the microscopic analysis of the nuclear wobbling motion. The main aim of this Letter is to analyze new data on high spin states in ^{156}Dy and ^{162}Yb [11,12] within a microscopic approach [13] based on the cranked Nilsson model plus random phase approximation (CRPA). In our approach mean-field parameters are determined from the energy-minimization procedure. The proper description of the moment inertia $\Im_x$ is achieved using the recipe suggested in Ref. [14]. Our calculations suggest that some excited states at high spins may represent wobbling excitations.

* Corresponding author at: Departament de Física, Universitat de les Illes Balears, E-07122 Palma de Mallorca, Spain.
E-mail address: rashid@theor.jinr.ru (R.G. Nazmitdinov).

0370-2693
doi:10.1016/j.physletb.2007.05.036

Our model Hamiltonian is

$$\hat{H}_\Omega = \hat{H}_0 - \sum_\tau \lambda_\tau \hat{N}_\tau - \Omega \hat{J}_x + V. \quad (1)$$

The term $\hat{H}_0 = \hat{H}_N + \hat{H}_{\rm add}$ contains the Nilsson Hamiltonian $\hat{H}_N$ and the additional term that restores the local Galilean invariance of the Nilsson potential, broken in the rotating frame [14]. This term is essential to obtain a correct description of $\Im_x$-moment of inertia [13]. Although the additional term $\hat{H}_{\rm add}$ breaks the rotational symmetry in the sense of Eq. (3) (see below), this effect can be negligibly small in the RPA order. The chemical potentials λ_τ ($\tau = n$ or p) are determined so as to give correct average particle numbers $\langle \hat{N}_\tau \rangle$. Hereafter, $\langle \ldots \rangle$ means the averaging over the mean field vacuum (yrast) state at a given rotational frequency Ω. The interaction V includes separable monopole pairing, monopole–monopole, and quadrupole–quadrupole terms to describe the positive parity states. All multipole and spin-multipole operators have a good isospin T and signature $r = \pm 1$ (see the properties of the matrix elements in Ref. [15]). They are expressed in terms of doubly stretched coordinates $\tilde{x}_i = (\omega_i/\omega_0)x_i$, which ensure the self-consistent conditions at the equilibrium deformation. Details about the model Hamiltonian (1) can be found in Ref. [13].

The Nilsson–Strutinsky analysis of experimental data on high spins in ^{156}Dy [12] indicates that the positive parity yrast sequence undergoes a transition from the prolate towards the oblate rotation. In our calculations the deformation parameters β and γ are defined by means of the oscillator frequencies $\omega_i^2 = \omega_0^2[1 - 2\beta\sqrt{\frac{5}{4\pi}}\cos(\gamma - \frac{2\pi}{3}i)]$ ($i = 1, 2, 3$ or x, y, z). To compare our results with available experimental data [12], we consider the mesh on the β, γ plane: from $\gamma = 60°$ (an oblate rotation around the y-axis) to $\gamma = -60°$ (an oblate rotation around the x-axis) and $\beta = 0$–0.6. At each rotational frequency, we have determined the equilibrium deformation parameters (β, γ) by minimizing the mean-field energy $E_{\rm MF} = \langle \hat{H}_\Omega - V \rangle$ on the mesh. In the vicinity of the backbending this procedure becomes highly unstable. In order to avoid unwanted singularities for certain values of Ω, we followed the phenomenological prescription [16] for the definition of the pairing gap parameter (see details in Ref. [13]). Parameters of the Nilsson potential were taken from Ref. [17]. In our calculations we include all shells up to $N = 9$. Near the transition point we extended our configuration space up to $N = 10$ shells. The difference between results from the former and the latter cases was small and all presented results are obtained with $N = 0$–9 shells. In contrast to standard calculations with the Nilsson potential, based on a "single stretched" coordinate method (cf. [18]), we use the real (non-stretched) ls and l^2 potentials, taking into complete account $\Delta N = 2$ mixing produced by them. This improves the accuracy of the mean-field calculations, since the "single stretched" ls and l^2 potentials break the rotational symmetry.

Our results conform to the results of the Nilsson + Strutinsky shell correction method (compare our Fig. 1 with Fig. 3c in Ref. [12]), although we obtain slightly different values for the equilibrium deformations. In the analysis of Ref. [12] the pairing correlations are missing, while the hexadecapole deformation is not included in the present calculations. The triaxiality of the mean-field sets in at the critical rotational frequency $\hbar\Omega_c$ which triggers the backbending in the considered nuclei due to different mechanisms. We obtain $\hbar\Omega_c \approx 0.25$ MeV ($10\hbar \to 12\hbar$) and $\hbar\Omega_c \approx 0.3$ MeV ($14\hbar \to 16\hbar$) for ^{162}Yb and ^{156}Dy, respectively. The contribution of the additional term was crucial to achieve a good correspondence between the calculated and experimental values of the crossing frequency in each nucleus. In ^{156}Dy we obtain that the γ-vibrational excitation ($K = 2$) of the positive signature tends to a zero in the rotating frame at the transition point, in close agreement with experimental data. At the transition point there are two indistinguishable mean-field energy minima with different shapes: axially symmetric and strongly nonaxial. The increase of the rotational frequency changes the axial shape to the nonaxial one with a negative γ-deformation ($\gamma \sim -20°$). In contrast with ^{156}Dy, in ^{162}Yb the axially symmetric configuration is replaced by the two-quasiparticle one with a small negative γ-deformation. There, the backbending occurs due to the rotational alignment of a neutron $i_{13/2}$ quasiparticle pair. The nonaxiality evolves quite smoothly.

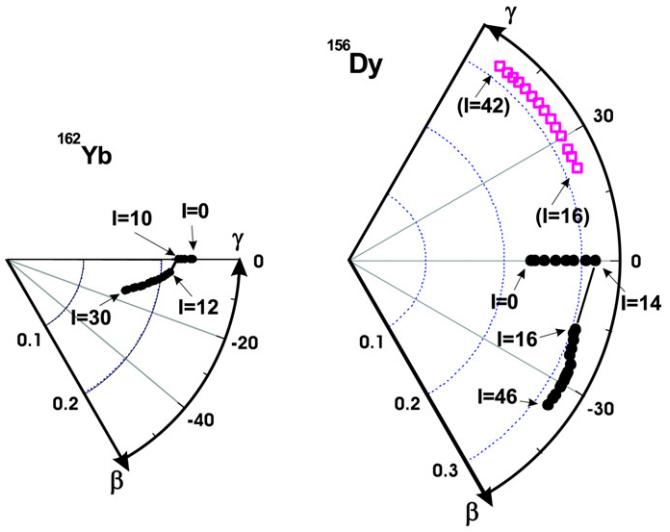

Fig. 1. Equilibrium deformations in β–γ plane as a function of the angular momentum $I = \langle \hat{J}_x \rangle - 1/2$ (in units of $\hbar$). The equilibrium deformations for ^{156}Dy provide the lower mean field energies in the region $-\pi/3 < \gamma < 0$ (filled circles) in comparison with those (open squares) obtained in Ref. [13]. The maximal difference between the minimal energies at the positive and negative equilibrium γ-values does not exceed ~ 1 MeV for ^{156}Dy.

In the CRPA approach the positive ($r = +1$) and negative ($r = -1$) signature boson spaces are not mixed, since the corresponding operators commute and $H_\Omega = H_\Omega(r = +1) + H_\Omega(r = -1)$. The self-consistency between the mean-field and the RPA calculations is achieved by varying the strength constants of the pairing and multipole interactions in the RPA. It results in the separation of collective excitations from those, related to the symmetries broken by the mean field. Two zero solutions are associated with the violation of the particle number (for protons and for neutrons) $[\hat{H}_\Omega(r = +), \hat{N}_\tau] = 0$. The other one is related to the spherical symmetries of the mean

field $[\hat{H}_\Omega(r=+), \hat{J}_x]=0$. While the positive signature excitations are analyzed in Ref. [13], the main focus of this Letter is wobbling excitations that belong to the negative signature sector. The negative signature RPA Hamiltonian has the form

$$\hat{H}_\Omega[r=-1]=\frac{1}{2}\sum_\mu E_\mu b^+_\mu b_\mu-\frac{\chi}{2}\sum_{\mu_3=1,2}\tilde{Q}^{(-)2}_{\mu_3}, \tag{2}$$

where $E_\mu=\varepsilon_i+\varepsilon_j$ ($E_{\bar{i}\bar{j}}=\varepsilon_{\bar{i}}+\varepsilon_{\bar{j}}$) are two-quasiparticle energies and $b^+_\mu(b_\mu)$ is a quasi-boson creation (annihilation) operator [13]. Hereafter, the index μ runs over ij, $\bar{i}\bar{j}$ and the index μ_3 is a projection on the quantization axis z. The double stretched quadrupole operators $\tilde{Q}^{(-)}_1=\xi\hat{Q}^{(-)}_1$ ($\xi=\omega_x\omega_z/\omega_0^2$), $\tilde{Q}^{(-)}_2=\eta\hat{Q}^{(-)}_2$ ($\eta=\omega_x\omega_y/\omega_0^2$) are defined by means of the quadrupole operators $\hat{Q}^{(r)}_m=i^{2+m+(r+3)/2}(\hat{Q}_{2m}+(-1)^{(r+3)/2}\hat{Q}_{2-m})/\sqrt{2(1+\delta_{m0})}$, where $\hat{Q}_{\lambda m}=\hat{r}^\lambda Y_{\lambda m}$ ($m=0,1,2$). The symmetry broken by the external rotational field (the cranking term) implies

$$[H_\Omega, \hat{J}_y\mp i\hat{J}_z]=\pm\Omega(\hat{J}_y\mp i\hat{J}_z) \tag{3}$$

(hereafter, we use in all equations $\hbar=1$). This condition is equivalent to the condition of the existence of the negative signature solution $\omega_\nu=\Omega$ created by the operator $\hat{\Gamma}^\dagger=(\hat{J}_z+i\hat{J}_y)/\sqrt{2\langle\hat{J}_x\rangle}$ [19]. We recall that $\hat{H}_{\rm add}$ in $\hat{H}_0$ (Eq. (1)) breaks Eq. (3) in general. However, to meet the condition (3) we determine the strength constant from the requirement of the existence of the RPA solution $\omega_\nu=\Omega$. As a result, the violation is unessential (see below).

We solve the RPA equations of motion for normal modes $[\hat{H}_\Omega, \hat{O}^\dagger_\nu]=\omega_\nu\hat{O}^\dagger_\nu$ with $\hat{O}^\dagger_\nu=\sum_\mu(\psi^{(\nu)}_\mu b^+_\mu-\phi^{(\nu)}_\mu b_\mu)$ (cf. [13]). The solution leads to a couple of equations for unknown coefficients

$$\tilde{R}^\nu_1=-\frac{1}{\sqrt{2}}[\hat{O}_\nu, \tilde{Q}^{(-)}_1], \qquad \tilde{R}^\nu_2=\frac{i}{\sqrt{2}}[\hat{O}_\nu, \tilde{Q}^{(-)}_2]. \tag{4}$$

Resolving these equations one obtains the secular equation

$$F(\omega_\nu)=\det\left(\mathbf{D}-\frac{\mathbf{1}}{\chi}\right)=0 \tag{5}$$

that determines all negative signature RPA solutions ω_ν. The matrix elements $D_{km}(\omega_\nu)=\sum_\mu \tilde{f}_{k,\mu}\tilde{f}_{m,\mu}C^{km}_\mu/(E^2_\mu-\omega^2_\nu)$ involve the coefficients $C^{km}_\mu=\omega_\nu$ for $k\neq m$ and E_μ otherwise; $\tilde{f}_{m,\mu}$ are two-quasiparticle matrix elements of operators $\tilde{Q}^{(-)}_m$. Among collective solutions there are solutions that correspond to the shape fluctuations of the system and the rotational mode $\omega_\nu=\Omega$. With aid of Eq. (3) the system for the unknown coefficients $\tilde{R}^\nu_{1,2}$ can be cast in the form similar to the classical expression for the wobbling mode

$$\omega_{\nu=w}=\Omega\sqrt{\frac{[\Im_x-\Im^{\rm eff}_2][\Im_x-\Im^{\rm eff}_3]}{\Im^{\rm eff}_2\Im^{\rm eff}_3}} \tag{6}$$

with microscopic effective moments of inertia [7]

$$\Im^{\rm eff}_{2,3}=\Im_{y,z}+\Omega S\frac{\Im_x-\Im_{y,z}-\omega^2_\nu S/\Omega}{\Im_{z,y}+\Omega S} \tag{7}$$

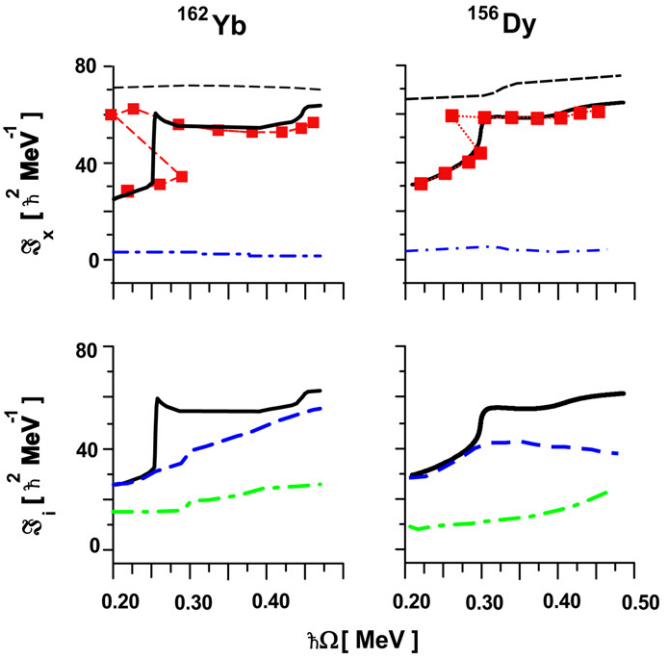

Fig. 2. Top panels: the kinematic $\Im_x=\langle\hat{J}_x\rangle/\Omega$ (solid line), the rigid body $\Im^{(\rm rig)}_1=\frac{2}{5}mAR^2(1-\sqrt{\frac{5}{4\pi}}\beta\cos(\gamma-\frac{2\pi}{3}))$ (dashed line) and the hydrodynamical $\Im^{(\rm irr)}_1=\frac{3}{2\pi}mAR^2\beta^2\sin^2(\gamma-\frac{2\pi}{3})$ (dash-dotted line) moments of inertia are compared with the experimental values (filled squares). Experimental values $\Im_x=I/\Omega$ are connected by dashed line to guide eyes ($\hbar\Omega=E_\gamma/2$). Bottom panels display the rotational dependence of the kinematic moment of inertia (solid line), effective moments of inertia $\Im^{\rm eff}_2$ (dashed line) and $\Im^{\rm eff}_3$ (dash-dotted line) for the first RPA solution $\nu=1$ obtained from Eq. (5).

that depend on the RPA frequency. Here, $\Im_x=\langle\hat{J}_x\rangle/\Omega$, $S=\sum_\mu J^y_\mu J^z_\mu/(E^2_\mu-\omega^2_\nu)$ and $\Im_{y,z}=\sum_\mu E_\mu(J^{y,z}_\mu)^2/(E^2_\mu-\omega^2_\nu)$. Eq. (6) does not contain the solution $\omega_\nu=\Omega$.

We obtain quite a remarkable correspondence between the experimental and calculated values for the kinematic moment of inertia for both nuclei (see top panels in Fig. 2). The irrotational fluid moment of inertia $\Im^{(\rm irr)}_1$ does not reproduce neither the rotational dependence nor the absolute values of the experimental one as a function of equilibrium deformations (see Fig. 2). The rigid body values provide the asymptotic limit of fast rotation without pairing, if shell effects are smeared out (see discussion on shell effects at fast rotation in Ref. [20]). Evidently, the difference between the rigid body and the calculated kinematic moments of inertia in both nuclei decreases with the increase of the rotational frequency, although it remains visible at high spins. At very fast rotation $\hbar\Omega>0.45$ MeV the pairing correlations are reduced due to multiple alignments, and, therefore, the difference is moderated. It is evident that for the rotation around the axis x the wobbling excitations with different collectivity could be found from Eq. (6), if $\Im_x>\Im^{\rm eff}_2, \Im^{\rm eff}_3$ (or $\Im_x<\Im^{\rm eff}_2, \Im^{\rm eff}_3$). The rotational behavior of the effective moments of inertia for the first RPA solution of Eq. (5) (see Fig. 2) suggests that this solution may be associated with a wobbling mode.

To identify the wobbling mode among the solutions of Eq. (5) it is instructive to introduce new variables, similar to

ones in [5]: $r_1^\nu = \tilde{R}_1^\nu/(\xi A)$, $r_2^\nu = \tilde{R}_2^\nu/(\eta B)$, where $A = \langle \hat{Q}_2 + \sqrt{3}\hat{Q}_0\rangle$, $B = 2\langle \hat{Q}_2\rangle$. By means of Eqs. (4) and $\hat{O}_{\nu=\Omega} \equiv \hat{\Gamma}$, we obtain exact definitions for the unknowns $r_{1,2}^\Omega$ associated with the redundant mode $\omega_\nu = \Omega$: $r_1^\Omega = -1/2\sqrt{\langle \hat{J}_x\rangle}$, $r_2^\Omega = 1/2\sqrt{\langle \hat{J}_x\rangle}$. With aid of these definitions, exploiting the fact that the components of the quadrupole tensor commute, one can define the unknowns

$$r_1^w = \frac{1}{2\sqrt{\langle \hat{J}_x\rangle}}\left(\frac{W_2}{W_3}\right)^{1/4}, \qquad r_2^w = \frac{1}{2\sqrt{\langle \hat{J}_x\rangle}}\left(\frac{W_3}{W_2}\right)^{1/4} \tag{8}$$

and show (cf. Ref. [5]) that they are associated with the wobbling mode. Here, $W_2 = (1/\Im_2^{\rm eff} - 1/\Im_x)$, $W_3 = (1/\Im_3^{\rm eff} - 1/\Im_x)$. It is convenient to use the variables $c_\nu = 4\langle \hat{J}_x\rangle r_1^\nu r_2^\nu$. From the definitions of $r_{1,2}^\Omega$, $r_{1,2}^w$ it follows that

$$c_{\nu=\Omega} \equiv -1, \qquad c_{\nu=w} \equiv 1. \tag{9}$$

Solving *only* the secular equation for the quadrupole operators, Eq. (5), the condition (9) enables us to identify the redundant and the wobbling modes. Note that the variables $r_{1,2}^\nu$ (or c_ν) can be only defined for nonaxial shapes.

The experimental level sequences for all observed up-to-date rotational bands in ^{162}Yb and ^{156}Dy are taken from Ref. [11]. All rotational states are classified by quantum number α which is equivalent to our signature r. The negative signature states ($r = -1$) correspond to $\alpha = 1$ and are associated with odd spin states in even–even nuclei. All considered bands are of the positive parity $\pi = +$. To elucidate the structure of observed states, we define the experimental excitation energy in the rotating frame $\hbar\omega_\nu(\Omega)_{\rm exp} = R_\nu(\Omega) - R_{\rm yr}(\Omega)$ as a function of the rotational frequency Ω [21]. Here, the Routhian function $R_\nu(\Omega) = E_\nu(\Omega) - \hbar\Omega I_\nu(\Omega)$. The energy $\hbar\omega_\nu(\Omega)_{\rm exp}$ can be compared with the RPA results, $\hbar\omega_\nu(\Omega)$, calculated at a given rotational frequency.

Top panels of Fig. 3 display the redundant mode and four lowest RPA solutions of Eq. (5) as a function of the rotational frequency. We recall that these solutions are found at different equilibrium deformations (see Fig. 1). Indeed, in both nuclei the criteria (9) uniquely determines the redundant and the wobbling modes. In Fig. 3 the redundant mode is manifested as a straight line (see top panels), while the corresponding coefficient $c_\Omega = -1$ (see bottom panels). The redundant mode is separated clearly from the vibrational modes.

In ^{162}Yb it is known only one negative signature γ-vibrational state. The first RPA solution ($\nu = 1$) is a negative signature gamma-vibrational mode (with odd spins) till $\hbar\Omega \approx 0.28$ MeV. With the increase of the rotational frequency it is transformed to the wobbling mode at $\hbar\Omega \approx 0.32$ MeV (according to the criterion (9)). Our results for $\nu = 1$ solution may be used as a guideline for possible experiments on identification of the wobbling excitations near the yrast line. The first negative signature RPA solution in ^{156}Dy can be associated with the negative signature gamma-vibrational excitations with odd spins. After the transition from the axial to nonaxial rotation, at $\hbar\Omega \approx 0.3$ MeV, according to the criteria (9), the

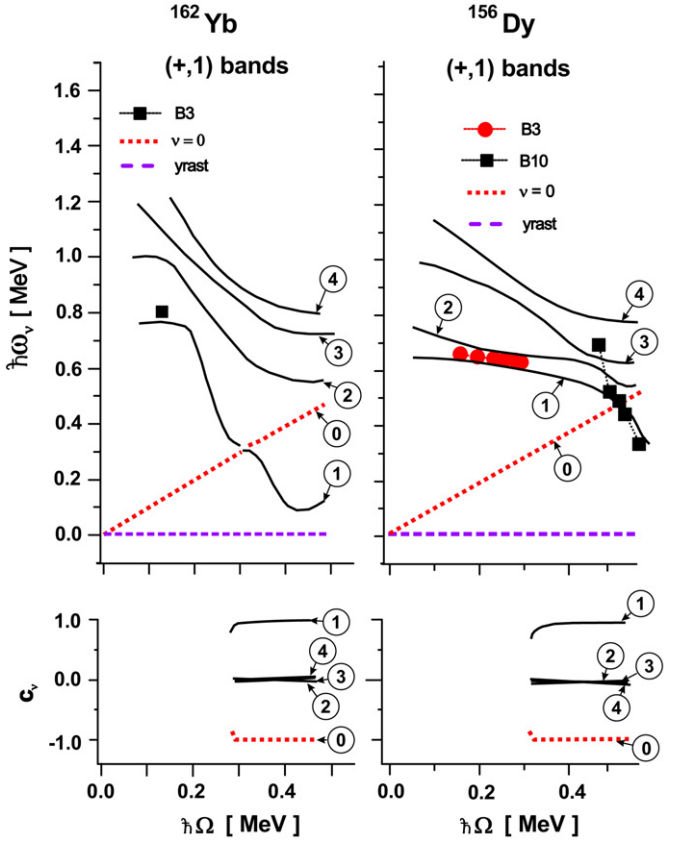

Fig. 3. Top panels: rotational dependence of the negative signature RPA solutions with odd spins ($\pi = +$, $\alpha = 1$). The redundant mode $\omega_\nu = \Omega$ is denoted as "0" and is displayed by the dotted line. Number in a circle denotes the RPA solution number: 1 is the first $\nu = 1$ RPA solution, etc. Different symbols display the experimental data associated with B1, B2, ... bands (the band labels are taken in accordance with the definitions given in Ref. [11]). Bottom panels: the rotational dependence of the coefficients $c_\nu \sim r_1^\nu r_2^\nu$ (see text) that are determined by the solutions of Eq. (5).

first negative signature RPA solution describes the wobbling excitations. The mode holds own features with the increase of the rotational frequency up to $\hbar\Omega \approx 0.55$ MeV. There is a good agreement (see Fig. 3, top right panel) between the RPA solution and the experimental Routhian of band B10 (or $(+,1)_1$ band according to Ref. [12]). On this basis we propose to consider the B10 band as the wobbling band in the range of values 0.45 MeV $< \hbar\Omega <$ 0.55 MeV ($33\hbar \leqslant I \leqslant 39\hbar$ for this band). Note that the band B10 contains the states with $31\hbar$–$53\hbar$. However, our conclusion is reliable only for the states with $I = 33\hbar$–$39\hbar$ (or up to $\hbar\Omega < 0.55$ MeV). At $\hbar\Omega \approx 0.55$ MeV a crossing of the negative parity and negative signature (positive simplex) B6 band with the yrast band B8 is observed. Therefore, for $\hbar\Omega > 0.55$ MeV (or for $I > 39\hbar$ for the B10 band) one may expect the onset of octupole deformation in the yrast states. The octupole deformation is beyond the scope of our analysis and will be discussed in forthcoming paper.

In the microscopic approach [5] the electric transition probabilities from the wobbling states take the same form as in the macroscopic rotor model [3]. Indeed, for interband transitions (from one-phonon to yrast states) we have (cf. [13,19])

$$B(\mathrm{E2}; I\nu \to I \pm 1\ \mathrm{yr}) \approx \left| \frac{i}{\sqrt{2}}[\tilde{O}_2^{(-)(E)}, \hat{O}_\nu^\dagger]/\eta \mp \frac{1}{\sqrt{2}}[\tilde{O}_1^{(-)(E)}, \hat{O}_\nu^\dagger]/\xi \right|^2. \quad (10)$$

Here, $\hat{M}^{(E)} = (eZ/A)\hat{M}$. In virtue of Eqs. (4), (8), one can obtain for the quadrupole transitions from the one-phonon wobbling state to the yrast states

$$B(\mathrm{E2}; Iw \to I \pm 1\ \mathrm{yr}) \approx \frac{1}{4\langle \hat{J}_x \rangle} \left| \left(\frac{W_2}{W_3}\right)^{\frac{1}{4}} A^{(E)} \mp \left(\frac{W_3}{W_2}\right)^{\frac{1}{4}} B^{(E)} \right|^2. \quad (11)$$

For intraband transitions we have (see [19] and Eq. (43) in Ref. [13])

$$B(\mathrm{E2}; I\nu \to I - 2\nu) \approx \frac{1}{8} \left| \sqrt{3}\langle \hat{Q}_0^{(E)} \rangle - \langle \hat{Q}_2^{(E)} \rangle \right|^2. \quad (12)$$

Expressions (10), (11), (12) are obtained in high spin limit $I \gg 1$. To understand a major trend of the quadrupole transitions, we employ relations from the pairing-plus-quadrupole model: $m\omega_0^2 \epsilon_2 \cos\gamma' = \chi\langle Q_0 \rangle$, $m\omega_0^2 \epsilon_2 \cos\gamma' = -\chi\langle Q_2 \rangle$ (cf. Ref. [2]). By means of these relations and a definition of the quadrupole isoscalar strength $\chi = 4\pi m\omega_0^2/5\langle r^2 \rangle \approx 4\pi m\omega_0^2/(3AR^2)$ ($R \approx 1.2A^{1/3}$ fm) one obtains from Eq. (11)

$$B(\mathrm{E2}; In_w = 1 \to I \pm 1\ \mathrm{yr}) \approx \frac{\Theta\epsilon_2^2}{\langle \hat{J}_x \rangle} \left[\left(\frac{W_2}{W_3}\right)^{\frac{1}{4}} \sin\left(\frac{\pi}{3} - \gamma'\right) \pm \left(\frac{W_3}{W_2}\right)^{\frac{1}{4}} \sin\gamma' \right]^2, \quad (13)$$

where $\Theta = (9/16\pi^2)e^2Z^2R^4$. Eq. (13) yields the following selection rules for the quadrupole transitions from the one-phonon wobbling band to the yrast one (for $W_{2,3} > 0$):

(a) $-60^\circ < \gamma < 0$:

$$B(\mathrm{E2}; In_w \to I - 1\ \mathrm{yr}) > B(\mathrm{E2}; In_w \to I + 1\ \mathrm{yr}),$$

(b) $0 < \gamma < 60^\circ$:

$$B(\mathrm{E2}; In_w \to I + 1\ \mathrm{yr}) > B(\mathrm{E2}; In_w \to I - 1\ \mathrm{yr}). \quad (14)$$

For the intraband transitions we obtain

$$B(\mathrm{E2}; In_w \to I - 2n_w) \approx \frac{1}{2}\Theta\epsilon_2^2 \cos^2\left(\frac{\pi}{6} - \gamma'\right). \quad (15)$$

One observes from Eq. (15) that for the transitions along the yrast line ($n_w = 0$) the onset of the positive (negative) values of γ-deformation leads to the increase (decrease) of the transition probability along the yrast line. Moreover, the decay from one-phonon wobbling states to the yrast line $R(\pm) = B(\mathrm{E2}; In_w = 1 \to I \pm 1\ \mathrm{yr})/B(\mathrm{E2}; In_w \to I - 2n_w) \sim 1/I$ ($\langle \hat{J}_x \rangle \approx I \gg 1$) decreases with the increase of the angular momentum for a constant deformation γ. However, the rotational evolution of the nonaxiality may affect this tendency. We predict almost a constant behavior for the ratio $R(-) \approx 0.1$ for both nuclei at $\hbar\Omega > 0.35$ MeV due to the increase of the nonaxial deformation.

At small rotational frequency, in both nuclei, transitions probabilities from the first one-phonon states are much weaker than quadrupole transitions along the yrast line (compare with Fig. 11 in Ref. [13]). At $\hbar\Omega \sim 0.05$ MeV the transition strength from the first one-phonon state to the yrast state: $\sim 330e^2$ fm^4 ($\sim 500e^2$ fm^4) in ^{162}Yb (^{156}Dy). We obtain a good correspondence between the shape evolution and the selection rules (14) for both nuclei (see top panels of Figs. 4 and 1). The transition probabilities, Eq. (10), are calculated by means of the $\psi_\mu^{(\nu)}$ and $\phi_\mu^{(\nu)}$ phonon amplitudes. The results for the first negative signature RPA solution (which is associated with a wobbling mode) are compared with those obtained with the aid of the effective moments of inertia (see Eqs. (7), (11)). Evidently, if the "spurious" solution (the redundant mode) would be not removed from Eq. (5), two estimations (10) and (11) (based on different secular equations (5) and (6), respectively) would produce different numerical values. A good agreement between both results (see Fig. 4) is the most valuable proof of the self-consistency of our calculations. The observed negligible differences are due to the approximate fulfillment of the conservation laws (3), caused by the additional term. In ^{162}Yb, starting from $\hbar\Omega \sim 0.28$ MeV (after the transition point), the negative signature phonon band changes the decay properties. The interband quadrupole transitions from the one-phonon state to the yrast ones with a lower spin dominate in the decay ($\Delta I = 1$, the case Eq. (14)(a)). Similar results for the first negative signature one-phonon band are obtained in ^{156}Dy. At low angular momenta ($\hbar\Omega \leqslant 0.3$ MeV) this band populates with approximately equal probabilities the

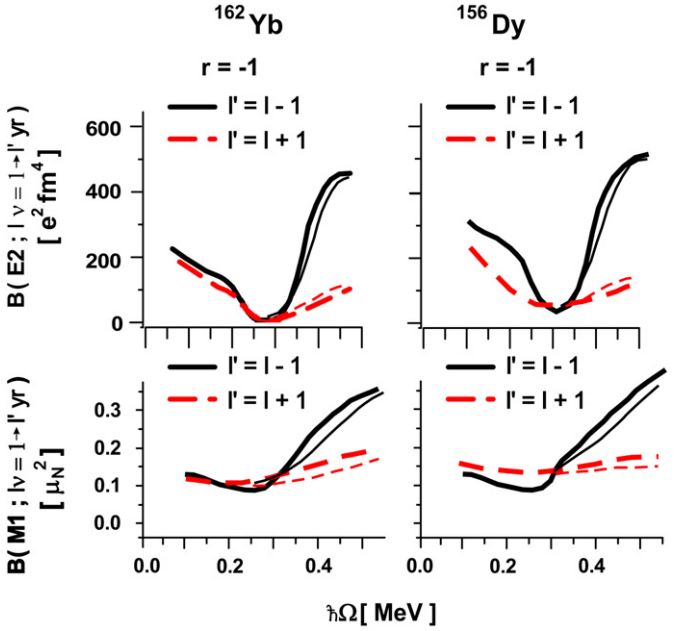

Fig. 4. B(E2)- (top) and B(M1)- (bottom) reduced transition probabilities from the one-phonon bands to the yrast band. The negative signature phonon band is described by the first RPA solution ($r = -1$). The transitions, calculated by means of the $\psi_\mu^{(\nu=1)}$ and $\phi_\mu^{(\nu=1)}$ phonon amplitudes, are connected by solid lines. The results obtained by means of Eqs. (11), (17) (with the aid of the variables $W_{2,3}$) are connected by thin lines, starting from the rotational frequency $\hbar\Omega \sim 0.3$ MeV. This point is associated in our analysis with the appearance of wobbling excitations. One observes a strong dominance of the B(E2)- and B(M1)-transitions from the wobbling states ($r = -1$) with spin I to the yrast states with spin $I' = I - 1$ starting from the rotational frequency $\hbar\Omega \geqslant 0.3$ MeV.

yrast states with $I' = I \pm 1$ (I is the angular momentum of the excited state). At $\hbar\Omega \sim 0.3$ MeV a shape-phase transition occurs, that leads to the triaxial shapes with the negative γ-deformation. In turn, the phonon band decays stronger on the yrast states with angular momenta $I' = I - 1$ ($\Delta I = 1$, the case Eq. (14)(a)), starting from $\hbar\Omega \geqslant 0.32$ MeV.

In the CRPA the magnetic transitions are defined as (cf. [19, 22])

$$B(\mathrm{M1}; I\nu \to I \pm 1\ \mathrm{yr}) \approx \frac{1}{2}\left|i\left[\hat{M}^{(M)}_{1\mu_3=1}, \hat{O}^{\dagger}_{\nu}\right] \mp \left[\hat{M}^{(M)}_{1\mu_3=0}, \hat{O}^{\dagger}_{\nu}\right]\right|^2. \quad (16)$$

Here, $\hat{M}^{(M)}_{1\mu_3} = \mu_N\sqrt{3}\sum_{i=1}^{A}(\frac{1}{2}g_s^{(i,\mathrm{eff})}[\sigma \otimes Y_{l=0}]_{1\mu_3} + g_l^{(i,\mathrm{eff})}[l \otimes Y_{l=0}]_{1\mu_3})$ is a magnetic dipole operator; μ_N is the nucleon magnetons, $g_s^{(\mathrm{eff})}$, $g_l^{(\mathrm{eff})}$ are the spin and orbital effective gyromagnetic ratios, respectively. Our results evidently demonstrate the dominance of $B(\mathrm{M1}; In_W \to I - 1\ \mathrm{yr})$ (see bottom panels in Fig. 4) in both nuclei. In the rigid rotor model, one can obtain for the magnetic transitions from the wobbling to yrast states

$$B(\mathrm{M1}; I\nu \to I \pm 1\ \mathrm{yr}) \approx \frac{1}{4\langle \hat{J}_x\rangle}\frac{(\sqrt{W_3} \mp \sqrt{W_2})^2}{\sqrt{W_2 W_3}}\left|\langle \hat{M}^{(M)}_{1\nu_3=1}[r=+1]\rangle\right|^2. \quad (17)$$

The full derivation will be presented elsewhere. Note that the dipole magnetic moment $\langle \hat{M}^{(M)}_{1\nu_3=1}[+]\rangle$ increases quite drastically, if a nucleus is undergoing the backbending [22]. For the wobbling states with $W_{2,3} > 0$, Eq. (17) yields

$$B(\mathrm{M1}; In_W \to I - 1\ \mathrm{yr}) > B(\mathrm{M1}; In_W \to I + 1\ \mathrm{yr}). \quad (18)$$

At high spin limit $I \gg 1$, the microscopic and rigid body values of the variables $W_{2,3}$ are very close. Thus, the macroscopic model supports the results of microscopic calculations for the magnetic transitions. It appears that the magnetic transitions with $\Delta I = 1\hbar$ always dominate from the wobbling to the yrast states, independently from the sign of the γ-deformation of rotating nonaxial nuclei.

In summary, we predict that the lowest excited negative signature and positive parity band in ^{162}Yb transforms to the wobbling band at $\hbar\Omega \sim 0.3$ MeV. We found that at $\hbar\Omega > 0.25$ MeV strong E2-transitions from this band start to populate yrast states, with the branching ratio $B(\mathrm{E2}; Iw \to I - 1\ \mathrm{yr})/B(\mathrm{E2}; Iw \to I + 1\ \mathrm{yr}) > 1$. Similar transition occurs in ^{156}Dy after the backbending as well, at $\hbar\Omega > 0.3$ MeV. A good agreement between our results and experimental Routhians allows us to conclude that the experimental states, associated with $(+,1)_1$ band in ^{156}Dy [12], are wobbling excitations at the rotational frequency values 0.45 MeV $< \hbar\Omega <$ 0.55 MeV. These states fulfill all requirements, specific for the wobbling excitations of rotating triaxial nuclei with the negative γ-deformation. It is quite desirable, however, to measure the interband B(E2)-transitions to draw a definite conclusion and we hope it will done in future. We predict the dominance of $\Delta I = 1\hbar$ magnetic transitions from the wobbling to the yrast states, independently from the sign of the γ-deformation.

Acknowledgements

We wish to thank the reviewer for his suggestions which helped to improve the clarity of the text and our analysis. This work is a part of the research plan MSM 0021620859 supported by the Ministry of Education of the Czech Republic and by the project 202/06/0363 of Czech Grant Agency. It is also partly supported by Grant No. FIS2005-02796 (MEC, Spain). R.G.N. gratefully acknowledges support from the Ramón y Cajal programme (Spain).

References

[1] E.S. Paul, et al., Phys. Rev. Lett. 98 (2007) 012501.
[2] S. Frauendorf, Rev. Mod. Phys. 73 (2001) 463.
[3] A. Bohr, B.R. Mottelson, Nuclear Structure, vol. II, Benjamin, New York, 1975.
[4] I.N. Mikhailov, D. Janssen, Phys. Lett. B 72 (1978) 303; D. Janssen, et al., Phys. Lett. B 79 (1978) 347.
[5] Y.R. Shimizu, M. Matsuzaki, Nucl. Phys. A 588 (1995) 559.
[6] D. Janssen, I.N. Mikhailov, Nucl. Phys. A 318 (1979) 390.
[7] E.R. Marshalek, Nucl. Phys. A 331 (1979) 429.
[8] S.W. Ødegård, et al., Phys. Rev. Lett. 86 (2001) 5866; D.R. Jensen, et al., Phys. Rev. Lett. 89 (2002) 142503; G. Schönwasser, et al., Phys. Lett. B 552 (2003) 9; H. Amro, et al., Phys. Lett. B 553 (2003) 197; A. Görgen, et al., Phys. Rev. C 69 (2004) 031301(R).
[9] I. Hamamoto, Phys. Rev. C 65 (2002) 044305.
[10] M. Matsuzaki, Y.R. Shimizu, K. Matsuyanagi, Phys. Rev. C 69 (2004) 034325.
[11] http://www.nndc.bnl.gov/nudat2/.
[12] F.G. Kondev, et al., Phys. Lett. B 437 (1998) 35.
[13] J. Kvasil, R.G. Nazmitdinov, Phys. Rev. C 69 (2004) 031304(R); J. Kvasil, R.G. Nazmitdinov, Phys. Rev. C 73 (2006) 014312.
[14] T. Nakatsukasa, et al., Phys. Rev. C 53 (1996) 2213.
[15] J. Kvasil, et al., Phys. Rev. C 58 (1998) 209.
[16] R. Wyss, et al., Nucl. Phys. A 511 (1990) 324.
[17] A.K. Yain, et al., Rev. Mod. Phys. 62 (1990) 393.
[18] S.G. Nilsson, et al., Nucl. Phys. A 131 (1969) 1.
[19] E.R. Marshalek, Nucl. Phys. A 275 (1977) 416.
[20] M.A. Deleplanque, et al., Phys. Rev. C 69 (2004) 044309.
[21] R.G. Nazmitdinov, Yad. Fiz. 46 (1987) 732, Sov. J. Nucl. Phys. 46 (1987) 412.
[22] J. Kvasil, et al., Phys. Rev. C 69 (2004) 064308.